Polyhedron 179 (2020) 114376

Contents lists available at ScienceDirect

Polyhedron

journal homepage: www.elsevier.com/locate/poly

Structure-property studies of a new one-dimensional Fe(III)/Mn(II) chain

Yuan-Zhu Zhang [a], Nigam P. Rath [a,b], John M. Cain [c], Mark W. Meisel [d], Stephen M. Holmes [a,b,*]

[a] Department of Chemistry and Biochemistry, University of Missouri-St. Louis, St. Louis, MO 63121, USA
[b] Center for Nanoscience, University of Missouri-St. Louis, St. Louis, MO 63121, USA
[c] Department of Chemistry, University of Florida, Gainesville, FL 32611-7200, USA
[d] Department of Physics and National High Magnetic Field Laboratory, University of Florida, Gainesville, FL 32611-8440, USA

ARTICLE INFO

Article history:
Received 25 October 2019
Accepted 16 January 2020
Available online 18 January 2020

Keywords:
Cyanometalates
Crystal structures
Magnetic properties
Polynuclear complexes

ABSTRACT

The preparation, structure, and magnetic properties of a one-dimensional chain, $\{[(pzTp)Fe^{III}(CN)_3][Mn^{II}(phen)_2][ClO_4]\}_n$ (**1**), are described. It is readily obtained from methanolic solutions containing $[NEt_4][(pzTp)Fe^{III}(CN)_3]\cdot H_2O$, $Mn^{II}(ClO_4)\cdot 6H_2O$, and two equivalents of 9,10-phenanthroline. Magnetic data indicate that the low spin Fe^{III}_{LS} (S = ½) and high spin Mn^{II}_{HS} (S = $^5/_2$) ions experience weak cyanide-mediated antiferromagnetic exchange [J_{iso} = −0.92(1) cm^{-1} and g_{iso} = 2.06(2)] owing to the presence of highly distorted $Fe^{III}(\mu$-CN)Mn^{II} units.

1. Introduction

Low-dimensional materials continue to remain of interest throughout the world-wide community owing to the range of properties displayed. Among highly tunable analogues are those derived from cyanometalates as they continue to offer a rich landscape for the systematic study of self-assembly processes, their structures, and magnetic properties within a given structural archetype. Poly(pyrazolyl)borate building blocks such as $[(Tp^R)Fe^{III}_{LS}(CN)_3]^-$ are attractive precursors for magnetic chain construction owing to their ability to exhibit first-order orbital contributions to their S = ½ spin ground states ($2.4 \leq g \leq 2.9$) [1–18]. These well-defined molecule-based complexes generally undergo selective self-assembly reactions to afford products whose nuclearity, numbers and orientation of formed M(μ-CN)M′ linkages, and properties are strongly correlated with the steric demand of their ancillary ligands [1–3,19–22]. These versatile, magnetically anisotropic, and highly tunable pyrazolylborate cyanometalates may be incorporated into a variety of discrete polynuclear complexes and chains that display single-molecule [1–14,16,17,23–25] and single-chain magnetic [25–29], solvent-assisted rearrangement and gas sorption [30,31], and photomagnetic [28,29,32–39] behavior.

The first cyanometalate to display thermo- and photochromic behavior, $K_{0.2}Co_{1.4}[Fe(CN)_6]\cdot 6.9H_2O$, was originally described by Hashimoto in 1996 [40]. The color and magnetism changes seen are a direct result of electron transfer where diamagnetic $\{Fe^{II}_{LS}(\mu$-CN)$Co^{III}_{LS}\}$ linkages are reversibly converted into paramagnetic $\{Fe^{III}_{LS}(\mu$-CN)$Co^{II}_{HS}\}$ ones at *ca.* 250 K [40–45]. Subsequent reports indicate that a variety of bistable cyanide-bridged complexes [32–39], chains [28,29], thin films and core–shell materials [46–51], may also be engineered to mimic behavior seen for the three-dimensional lattice.

A second structurally related solid, $RbMn[Fe(CN)_6]\cdot H_2O$, is also known to exhibit optical and magnetic bistability that is reminiscent of the better known Fe/Co Prussian blues [52–58]. In these analogues valence tautomeric $\{Fe^{II}_{LS}(\mu$-CN)$Mn^{III}_{HS}\}$ units are reversibly converted into $\{Fe^{III}_{LS}(\mu$-CN)$Mn^{II}_{HS}\}$ ones with increasing temperature or upon light exposure. The structural changes that accompany electron transfer also induces a tetragonal to cubic phase transformation, as conversion of Jahn-Teller distorted Mn^{III}_{HS} to Mn^{II}_{HS} ions occurs [52–58].

Surprisingly, while numerous complexes are known to mimic optical and magnetic bistability seen in Fe/Co Prussian blue analogues, no molecule-based complexes or chains containing bistable Fe/Mn pairs are currently known [5,8,59–67]. As part of a continuing effort to better understand how to manipulate the optical and magnetic properties of low-dimensional materials, our attention turned towards the preparation of tunable one-low-dimensional $\{FeMn\}_n$ networks that may undergo electron transfer. The results of these efforts are reported below.

2. Experimental

2.1. General considerations

All operations were conducted under an argon atmosphere using standard Schlenk and dry box techniques. Solution transfers

* Corresponding author at: Department of Chemistry and Biochemistry, University of Missouri-St. Louis, St. Louis, MO 63121, USA.
E-mail address: holmesst@umsl.edu (S.M. Holmes).

https://doi.org/10.1016/j.poly.2020.114376
0277-5387/

utilized stainless steel cannulas. The preparation of $[NEt_4][(pzTp)Fe(CN)_3]\cdot H_2O$ is described elsewhere [7,8]. Methanol (MeOH) was distilled under dinitrogen from magnesium turnings and sparged with argon prior to use. Elemental analyses were performed by Robertson Microlit Laboratories.

Caution! Perchlorate salts and their derivatives are potentially explosive. They may be thermally, shock, and friction sensitive. Although no problems were encountered during our studies cyanides and perchlorates are toxic and should be handled with care.

2.2. Preparation of $\{[(pzTp)Fe(CN)_3][Mn(phen)_2][ClO_4]\cdot{}^1/_4H_2O\}_n$ (**1**)

Solid phen (73.5 mg, 0.408 mmol) was dissolved into MeOH (5 mL) with stirring and was quickly added to a methanolic solution (5 mL) of $Mn(ClO_4)_2\cdot 6H_2O$ (72.5 mg, 0.200 mmol). After 30 min. a MeOH (10 mL) solution of $[NEt_4][(pzTp)Fe(CN)_3]\cdot H_2O$ (108.5 mg, 0.193 mmol) was added affording a dark red solution. The mixture was filtered and allowed to stand for 7 d at room temperature (28). The dark red plates were collected via suction filtration, washed with MeOH (5 mL), and dried under vacuum for 2 min. at room temperature. Yield: 145 mg (78.4%). Anal. Calcd for $C_{39}H_{30}BClFeMnN_{15}O_4$ (**1 – 1/4H$_2$O**): C, 50.49; H, 3.04; N, 22.65. Found: C, 50.43; H, 3.08; N, 22.52. IR (Nujol/KBr, cm^{-1}): 3567 (m), 3141 (m) 3063 (m) 2924 (vs) 2854 (vs) 2724 (w) 2153 (s), 2143 (s), 2122 (w), 1670 (w), 1578 (w), 1624 (vs), 1519 (s), 1500 (vs), 1458 (s), 1426 (s), 1408 (s), 1386 (s), 1377 (s), 1341 (w), 1296 (s), 1303 (s), 1341 (m), 1261 (m), 1210 (s), 1182 (m), 1144 (s), 1144 (vs), 1093 (vs), 1069 (vs), 967 (w), 922 (w), 859 (s), 848 (s), 806 (vs), 791 (s), 781 (s), 763 (s), 729 (s), 661 (w), 640 (w), 624 (s), 489 (w), 458 (w), 422 (m). UV–vis (Nujol/KBr): λ_{max}/nm 455 (m, sh), 525 (s, sh), 624 (vs), 643 (vs), 750 (m).

2.3. Spectroscopic and magnetic measurements

Infrared spectra were recorded as Nujol mulls between KBr plates on a Thermo-Fisher Nicolet Impact 6700 FTIR instrument in the 400–4000 cm^{-1} region. Variable temperature infrared data were collected using a liquid nitrogen cooled Janis ST-100 cryostat equipped with a LakeShore 331 temperature controller operating between 80 and 350 K. Variable temperature electronic spectra were obtained as Nujol mulls between Mylar films on a Janis EXOL cryostat equipped with a LakeShore 335 temperature controller (20–300 K range), CTI SC Cryo helium compressor and CTI M22 cold head, Ocean Optics Flame-S-UV–VIS-ES spectrophotometer, and a DH-2000-BAL balanced deuterium tungsten light source (200 to 850 nm range).

Magnetic measurements on a microcrystalline sample of **1** (22.2 mg) were collected on a Quantum Design MPMS-XL 7 magnetometer operating between 2 and 300 K and applied magnetic fields ranging between $-7 \leq 0 \leq 7$ T. The magnetic data were corrected for the sample holder and diamagnetic contributions were estimated using Pascal's constants [68]. Elemental analyses were performed by Robertson Microlit Laboratories. Magnetic data figures were generated using Origin 2019b (www.originlab.com).

2.4. Structural determinations and refinements

Single crystal structural data for **1** were collected at 100(2) K on a Bruker Apex-II CCD diffractometer using graphite-collimated MoK α (λ = 0.71073 Å) radiation. All crystals were mounted in Paratone-N oil on nylon loops. The structures were solved by direct methods (SHELXS97) [69,70] and completed by difference Fourier methods (SHELXL-2016) [69,70]. Refinement was performed against F^2 by weighted full-matrix least-squares (SHELXL-2016) [69,70] and empirical absorption corrections (SADABS) [71] were applied. Hydrogen atoms for **1** were found in difference maps and subsequently placed at calculated positions using suitable riding models with isotropic displacement parameters derived from their carrier atoms. Non-hydrogen atoms were refined with anisotropic displacement parameters. Atomic scattering factors were taken from the *International Tables for Crystallography Vol. C. 82* [72]. All figures were generated using CrystalMaker X® (CrystalMaker Software Ltd, www.crystalmaker.com).

3. Results and discussion

3.1. Synthesis and spectroscopic characterization

Treatment of a 1:1 ratio of tricyanoferrate(III) and $Mn(phen)_2^{2+}$ complexes in methanol readily affords the one-dimensional chain, $\{[(pzTpFe^{III}(CN)_3][Mn^{II}(phen)_2][ClO_4]\cdot{}^1/_4H_2O\}_n$ (1), where phen = 9,10-phenanthroline and pzTp = tetra(pyrazolyl)borate. The infrared spectrum of **1** displays two strong ν_{CN} cyanide stretching absorptions that are shifted to higher energies relative to the one seen for $[NEt_4][(pzTp)Fe^{III}(CN)_3]\cdot H_2O$ (2119 cm^{-1}) [7,8]. These high energy absorptions [2152 and 2144 cm^{-1}] are in the range expected for compounds containing $Fe^{III}_{LS}(\mu\text{-CN})Mn^{II}$ linkages, while a third one [2122 cm^{-1}] is ascribed to a terminal Fe-CN unit [1,3,5,7,8,14,59–67]. These cyano stretches resemble those seen in the infrared spectra of $RbMn[Fe(CN)_6]\cdot H_2O$ [2155 and 2164 cm^{-1}] for temperatures above *ca.* 250 K [52–58]. However at lower temperatures, the Fe/Mn Prussian blue analogue displays lower energy absorptions belonging to $Fe^{II}(\mu\text{-CN})Mn^{III}$ units [2086, 2091, 2110, and 2130 cm^{-1}], in addition to a single higher energy one [2202 cm^{-1}] ascribed to putative $Fe^{III}(\mu\text{-CN})Mn^{III}$ units [52–55]. Unfortunately, no changes in the infrared spectra of **1** were seen between 80 and 350 K in the absence or presence of white light (5 h), indicating that the Fe^{III}/Mn^{II} pairs are the preferred valence tautomeric state. Likewise, solid state variable-temperature UV–vis spectra collected for **1** as Nujol mulls or between Mylar films show intense and broad absorptions seen at *ca.* 624 and 643 nm that are reminiscent of those in $RbMn[Fe(CN)_6]\cdot H_2O$ [52–58]. However, these bands remain invariant with respect to changes in temperature or white light exposure, confirming that **1** does not exhibit thermo- or photochromism.

3.2. Crystallographic studies

Compound **1** crystallizes in the monoclinic $P2_1/n$ space group as a cationic one-dimensional sesquihydride chain (Table 1). The asymmetric unit contains a $[(pzTp)Fe^{III}(CN)_3]^-$ anion that is linked via a bridging cyanide to an adjacent $[Mn^{II}(phen)_2]^{2+}$ fragment, leaving a single terminal cyanide per iron center. A single charge-balancing and disordered perchlorate anion and fractionally occupied lattice water are also found in the interchain region of its structure. The terminal cyanide Fe1–C distance [Fe1–C14, 1.931(2) Å] is smaller than the bridging ones [Fe1–C13, 1.913(2); Fe1–C15, 1.909(2) Å] while the Fe-CN units are slightly bent, ranging between 173.4(2) to 178.4(2) Å for Fe1–C15–N11 and Fe1–C14–N10, respectively (Table 2). The $[Mn(phen)_2(\mu\text{-NC})_2]$ fragment adopts a distorted MnN_6 coordination environment due to extensive steric interactions between phen and pzTp ligands [Fig. 1, top]. The $Mn1–N_{cyanide}$ bonds for Mn1–N9A and Mn1–N11 [2.219 (2) and 2.167(2) Å] are slightly different while the $Mn1–N_{phen}$ ones are slightly longer, ranging between 2.221(1) and 2.313(1) Å, for Mn1–N12 and Mn1–N14, respectively. The $Mn1–NC_{cyanide}$ units are non-linear and are 142.8(1) and 169.5(1)°, for Mn1–N9–C13 and Mn1A–N11–C15, respectively [Fig. 1, bottom]. The N-Mn-N angles for the coordinated phenanthroline ligands are also rather acute [N12–Mn1–N13, 73.13(5)°; N14–Mn1–N15, 73.75(6)°] as is typically seen in a variety of $M(L)_2^{n+}$ complexes, where L = 2,2′-

Table 1
Crystallographic data for **1**.[a–c]

Formula	$C_{156}H_{114}B_4Cl_4Fe_4Mn_4N_{60}O_{17}$
Formula weight	3729.27
λ (Å)	0.71073
T (K)	100(2)
Crystal system	monoclinic
Space group	$P2_1/n$
a (Å)	13.7611(5)
b (Å)	10.5319(5)
c (Å)	27.226(1)
α (Å)	90
β (Å)	91.834(2)
γ (Å)	90
V (Å^3)	3943.8(3)
Z	1
ρ_{calcd} (mg m^{-3})	1.570
μ (mm^{-1})	0.821
R_1^b	0.0371
wR_2^c	0.0815

[a] $I \geq 2\sigma(I)$.
[b] $R_1 = \sum||F_o| - |F_c||/\sum|F_o|$.
[c] $wR_2 = \{\sum[w(F_o^2 - F_c^2)^2]/\sum[w(F_o^2)^2]\}^{1/2}$.

Table 2
Selected bond distances (Å) and angles (°) for **1**.

Fe1–C13	1.913(2)	C13–Fe1–C14	87.87(7)
Fe1–C14	1.931(2)	C13–Fe1–C15	90.78(7)
Fe1–C15	1.909(2)	C14–Fe1–C15	85.03(7)
Fe1–N1	1.975(1)	C13–Fe1–N1	178.92(6)
Fe1–N3	1.971(1)	C13–Fe1–N3	90.63(6)
Fe1–N5	1.949(1)	C13–Fe1–N5	91.23(6)
Mn1–N9A	2.219(2)	N1–Fe1–N3	88.35(6)
Mn1–N11	2.167(2)	N1–Fe1–N5	88.37(6)
Mn1–N12	2.221(1)	N3–Fe1–N5	88.34(5)
Mn1–N13	2.313(1)	N9A–Mn1–N11	86.53(5)
Mn1–N14	2.268(1)	N9A–Mn1–N12	92.19(5)
Mn1–N15	2.250(1)	N9A–Mn1–N13	163.09(5)
C13–N9	1.149(2)	N9A–Mn1–N14	82.94(5)
C14–N10	1.148(2)	N9A–Mn1–N15	103.27(5)
C15–N11	1.150(2)	N11–Mn1–N12	102.34(5)
		N11–Mn1–N13	88.45(5)
		N11–Mn1–N14	161.57(5)
		N11–Mn1–N15	94.15(6)
		N12–Mn1–N13	73.13(5)
		N14–Mn1–N15	73.75(6)
		Fe1–C13–N9	174.1(2)
		Fe1–C14–N10	178.4(2)
		Fe1–C15–N11	173.4(2)
		C13–N9–Mn1	142.8(1)
		C15–N11–Mn1A	169.5(1)

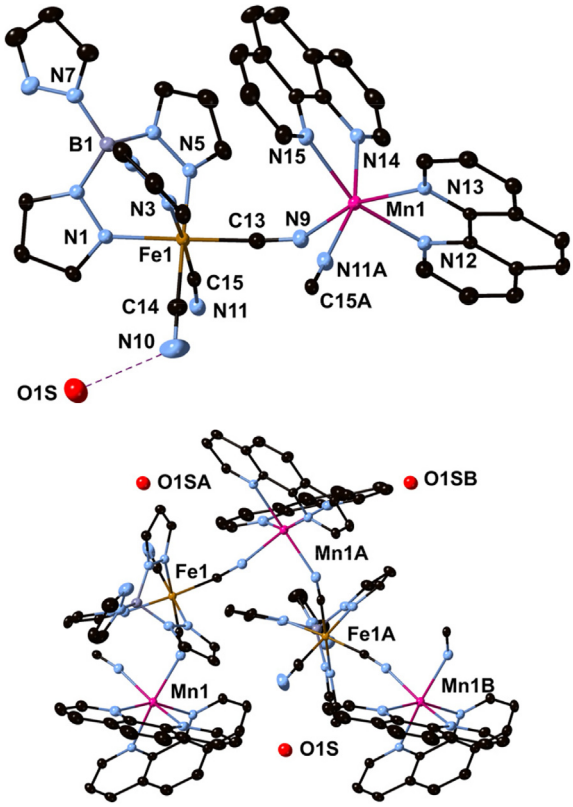

Fig. 1. (top) Asymmetric unit of **1**. Thermal ellipsoids are at the 50% level and hydrogen atoms and perchlorate anions are eliminated for clarity. Dotted line represents hydrogen bonding between fractionally occupied lattice water (O1S) and a terminal cyanide nitrogen atoms (N10). (bottom) Fragment of one-dimensional chain structure in **1** viewed along the crystallographic *a*-direction. Thermal ellipsoids are at the 50% level and hydrogen atoms and perchlorate anions are eliminated for clarity.

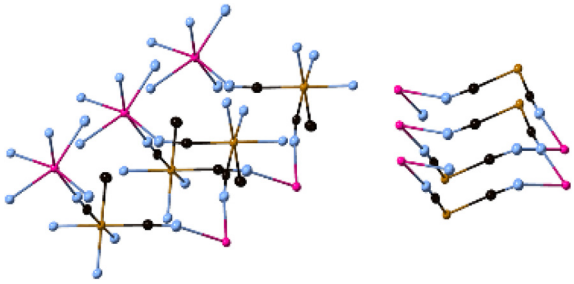

Fig. 2. (top) Truncated ball and stick view of **1** approximately along the crystallographic *b*-direction highlighting the twisting of the {Fe-CN-Mn}$_n$ chain where only C (black), N (blue), Fe (orange), and Mn (pink) atoms are shown for clarity. (bottom) Truncated view of **1** along the *b*-direction highlighting the helical cyanide-bridged {Fe-CN-Mn}$_n$ units within the chain. (For interpretation of the references to colour in this figure legend, the reader is referred to the web version of this article.)

bipyridine or 9,10-phenathroline [73–77]. The helical {Fe-CN-Mn}$_n$ units propagate along the crystallographic *b*-direction adopting a torsional angle of *ca.* 17.3° [Fig. 2].

We note that all but one of the hydrogen atoms were found in the difference maps of **1**. The fractionally occupied lattice water (O1S) was refined to be *ca.* ¼ per {FeMn}$_n$ repeat unit and is in close proximity to several ancillary ligands, the terminal cyanide (N10), and disordered perchlorate anion atoms (O4). The close contacts between terminal cyanides and lattice water [N10···O1S, 2.754 (1) Å] suggest hydrogen bonding may be operative [Fig. 1, top] while additional ones involving the Tp* [C1···O1S, 3.388(2) Å; C2···O1S, 4.102(2) Å], phen [C24···O1S, 3.210(2) Å; C28···O1S, 3.112(2) Å; C29···O1S, 3.286(2) Å], and disordered perchlorate anion [O4′···O1S, 3.936(2) Å; Cl1′···O1S, 3.842(2) Å] are also seen. We were unable to find any electron density ascribable to a hydrogen atom along the O4···H-O1S vector in the structure owing to the disordered nature of the charge balancing perchlorates and their geometric relationship to the O1S-H-N10 interaction. Assuming these close contacts are consequences of crystal packing, rather than bona fide hydrogen bonds, we elected to exclude this perchlorate O4/O4′···H···O1S(H_2O) contact from the structural description. Lastly, we note that these attributes are also found in the structure of one-dimensional {[Fe^{III}(bpb)$(CN)_2$][$Mn^{II}(L^1)$][ClO_4]}$_n$·$^1/_2H_2O$, where bpb^{2-} = 1,2-bis(pyridine-2-carboxamido)benzenate and L^1 = 3,6-diazaoctane-1,8-diamine [64].

3.3. Magnetic studies

At 300 K, the χT product for **1** is near the expected value for a 1:1 ratio (5.06 cm^3 K mol^{-1}] of magnetically non-interacting Fe^{III}_{LS}

($S = {}^1/_2$; $2.4 \leq g \leq 2.8$) and Mn^{II}_{HS} ($S = {}^5/_2$; $g \sim 2$) ions, if each site contributes *ca.* 0.68 and 4.4 cm^3 K mol^{-1}, respectively. However, the experimental χT product is actually lower [4.79 cm^3 K mol^{-1}], suggesting that spin–orbit contributions from the Fe^{III} ions are largely quenched. Curie-Weiss fits of χ^{-1} vs T data between 30 and 300 K gave a Weiss constant (θ) of −2.7(2) K [for C = 4.79(2) cm^3 K mol^{-1}] which is somewhat larger than that reported [θ = −1.73 K] for chains such as $\{[Fe^{III}(bpb)(CN)_2][Mn^{II}(L^1)][ClO_4]\}_n \cdot {}^1/_2H_2O$, where bpb^{2-} = 1,2-bis(pyridine-2-carboxamido)benzenate and L^1 = 3,6-diazaoctane-1,8-diamine [64].

The temperature dependence of the χT vs T data at an applied magnetic field of 1000 Oe clearly shows that compound **1** undergoes antiferromagnetic exchange between the iron and manganese sites [Fig. 3]. This behavior is consistent with both orbital symmetry and Goodenough-Kanamori arguments [78]. With decreasing temperatures, the χT product gradually approaches a minimum value [4.41 cm^3 K mol^{-1}] at 12 K, confirming local antiferromagnetic interactions are present [Fig. 3]. At lower temperatures, the χT values again increase towards a maximum of 8.00 cm^3 K mol^{-1} at 2.5 K. This behavior is reminiscent of that reported for several one dimensional $\{Fe^{III}_{LS}Mn^{II}_{HS}\}_n$ S = 2 chains [59–67]. The field dependence of the magnetization was measured at 2 and 5 K and the M vs H data clearly shows the chains are easily saturated and approach values of 4.80 μ_B at 2 K. The experimental value is close to the expected one [4.90 μ_B] assuming that $g_{iso} \sim 2.2$ for an antiferromagnetically coupled $\{Fe^{III}Mn^{II}\}_n$ chain [Inset of Fig. 3].

The χ vs T data were initially modeled following methods described by Ni and Jiang for one-dimensional $\{Fe^{III}Mn^{II}\}_n$ chains [64]. Assuming that an isotropic exchange Hamiltonian, $H = -2J[S_1 \cdot S_2]$, adequately describes the magnetic exchange interactions between the low spin Fe^{III}_{LS} and high spin Mn^{II}_{HS} ions, the susceptibility of the $\{Fe^{III}Mn^{II}\}$ repeat unit may be described via the following equations:

$$\chi_d = \frac{N_A g^2 \beta^2 S_d(S_d+1)(28+10\exp(-6J/k_gT))}{3k_BT(7+5\exp(-6J/k_BT))} \quad (1)$$

$$\chi_d = \frac{N_A g^2 \beta^2 (S_d+1)(1+u)}{3k_BT(1-u)} \quad (2)$$

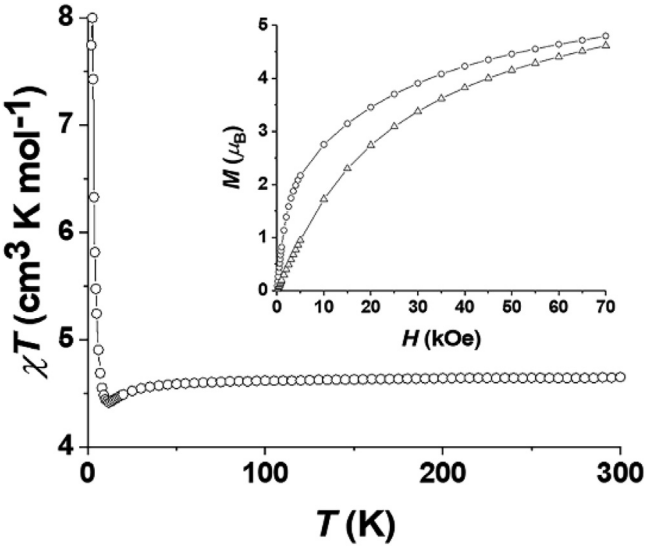

Fig. 3. Temperature dependence of the χT product for **1** under an static applied dc magnetic field of H = 1 kOe. Inset: Magnetic field dependence of the magnetization for data collected at 2 (○) and 5 (Δ) K. The solid lines are guides for the eye.

where $u = \coth(J_2S_d(S_d+1)/k_BT) - k_BT/J_2S_d(S_d+1)$. In the present case, g_{iso} (average g value for a $Fe^{III}Mn^{II}$ dimer) and J_1 were found to be 2.06(2) and −0.92(1) cm^{-1}, which is consistent with modest antiferromagnetic cyanide-mediated superexchange within the significantly bent $Fe^{III}(\mu\text{-CN})Mn^{II}$ units [59–67]. Additional intra- and interchain exchange interactions (J_2 and zJ) proved to be exceptionally small and were deemed to be physically meaningless. This behavior is reminiscent of Julve's 4,2-ribbons, $\{Fe^{III}(dmbpy)(CN)_4\}_2$-$Mn^{II}(H_2O)_2\}_n$, where dmbpy = 4,4′-dimethyl-2,2′-bipyridine [65]. However, in contrast to **1** and Julve's chain, MAGPACK [79,80] simulations of the χT vs T data collected for another double zig-zag chain, $\{[(Tp^*)Fe^{III}(CN)_3]_2[Mn^{II}(EtOH)_2]\cdot 4H_2O\}_n$, indicates that more efficient antiferromagnetic exchange interactions [J = −7.65 and g = 2.15] are operative when more anisotropic iron(III) ions and nearly linear $Fe^{III}(\mu\text{-CN})Mn^{II}$ linkages are present [67]. Overall, we conclude that the deduced magnetic parameters fall within the typical ranges reported for a variety of one-dimensional Fe^{III}/Mn^{II} networks [59–67].

4. Conclusions

In summary, the preparation, structure, and magnetic properties of a cyanide-bridged one-dimensional $\{Fe^{III}Mn^{II}\}_n$ chain are described. Owing to the presence of a highly bent $Fe(\mu\text{-CN})Mn$ linkages inefficient superexchange is found between the magnetic orbitals. The apparent absence of electron transfer in **1** is attributed to the highly distorted structure of the chains which provide an inadequate ligand field for oxidation of the manganese and concomitant reduction of the iron sites within the $Fe^{III}_{LS}(\mu\text{-CN})Mn^{II}_{HS}$ units.

CRediT authorship contribution statement

Yuan-Zhu Zhang: Methodology, Validation, Investigation, Resources. **Nigam P. Rath:** Methodology, Validation, Formal analysis, Investigation, Resources, Data curation, Writing - review & editing, Visualization, Supervision. **John M. Cain:** Conceptualization, Methodology, Validation, Investigation, Resources, Data curation. **Mark W. Meisel:** Methodology, Validation, Formal analysis, Investigation, Resources, Data curation, Writing - original draft, Supervision, Project administration, Funding acquisition. **Stephen M. Holmes:** Conceptualization, Methodology, Validation, Formal analysis, Investigation, Resources, Data curation, Writing - original draft, Writing - review & editing, Visualization, Supervision, Project administration, Funding acquisition.

Declaration of Competing Interest

The authors declare that they have no known competing financial interests or personal relationships that could have appeared to influence the work reported in this paper.

Acknowledgements

S.M.H. gratefully acknowledges the National Science Foundation (CHE-1214063 and CHE-1800578; CHE-0939987, X-ray upgrade) for financial support. M.W.M. and J.M.C. also thank the National Science Foundation (DMR-1708410) for additional funding support.

Appendix A. Supplementary data

Additional magnetic data is electronically available. CCDC 1956423 (**1**) contains the supplementary crystallographic data and may be obtained free of charge via the Internet at http://

www.ccdc.cam.ac.uk/conts/retrieving.html or from the Cambridge Crystallographic Data Centre, 12 Union Road, Cambridge CB2 1EZ, UK; fax: +44 1223 336 033 or e-mail: deposit@ccdc.cam.ac.uk. Supplementary data to this article can be found online at https://doi.org/10.1016/j.poly.2020.114376.

References

[1] P.J. Ferko, S.M. Holmes, Curr. Inorg. Chem. 3 (2013) 172, and references cited therein.
[2] Y.-Z. Zhang, U.P. Malik, B. Quiggins, H. Nguyen, C.C. Beedle, A.E. Kovalev, R. Clérac, S. Hill, B.J. Bythell, S.M. Holmes, Eur. J. Inorg. Chem. 24 (2016) 2432–2442.
[3] S. Wang, X.H. Ding, J.-L. Zuo, X.-Z. You, W. Huang, Coord. Chem. Rev. 255 (2011) 1713, and references cited therein.
[4] Y. Song, P. Zhang, X.-M. Ren, X.-F. Shen, Y.-Z. Li, X.-Z. You, J. Am. Chem. Soc. 127 (2005) 3708.
[5] D.F. Li, S. Parkin, G.B. Wang, G.T. Yee, A.V. Prosvirin, S.M. Holmes, Inorg. Chem. 44 (2005) 4903.
[6] Y.-Z. Zhang, U.P. Mallik, N.P. Rath, R. Clérac, S.M. Holmes, Inorg. Chem. 50 (2011) 10537.
[7] D.-F. Li, S. Parkin, G.B. Wang, G.T. Yee, R. Clérac, W. Wernsdorfer, S.M. Holmes, J. Am. Chem. Soc. 128 (2006) 4214.
[8] D.-F. Li, R. Clérac, S. Parkin, G.-B. Wang, G.T. Yee, S.M. Holmes, Inorg. Chem. 45 (2006) 5251.
[9] Y.-Z. Zhang, U.P. Mallik, N.P. Rath, G.T. Yee, R. Clérac, S.M. Holmes, Chem. Commun. 46 (2010) 4953.
[10] Y.-Z. Zhang, U.P. Mallik, R. Clérac, N.P. Rath, S.M. Holmes, Chem. Commun. 47 (2011) 7194.
[11] C.-F. Wang, W. Liu, Y. Song, X.-H. Zhou, J.-L. Zuo, X.-Z. You, Eur. J. Inorg. Chem. (2008) 717.
[12] C.-F. Wang, Z.-G. Gu, X.-M. Lu, J.-L. Zuo, X.-Z. You, Inorg. Chem. 47 (2008) 7957.
[13] W. Liu, C.-F. Wang, Y.-Z. Li, J.-L. Zuo, X.-Z. You, Inorg. Chem. 45 (2006) 10058.
[14] S. Wang, J.-L. Zuo, H.-C. Zhou, Y. Song, S. Gao, X.-Z. You, Eur. J. Inorg. Chem. (2004) 3681.
[15] Z.-G. Gu, Q.-F. Yang, X.-H. Zhou, J.-L. Zuo, X.-Z. You, Inorg. Chem. 46 (2007) 3236.
[16] L.M. Toma, R. Lescouezec, J. Pasan, C. Ruiz-Perez, J. Vaissermann, J. Cano, R. Carrasco, W. Wernsdorfer, F. Lloret, M. Julve, J. Am. Chem. Soc. 128 (2006) 4842.
[17] C.-F. Wang, D.-P. Li, X. Chen, X.-M. Li, Y.-Z. Li, J.-L. Zuo, X.-Z. You, Chem. Commun. 45 (2009) 6940.
[18] R. Lescouëzec, J. Vaissermann, F. Lloret, F. Julve, M. Verdaguer, Inorg. Chem. 41 (2002) 5943–5945.
[19] Nihei, M. Ui, N. Hoshino, H. Oshio, Inorg. Chem. 47 (2008) 6106.
[20] Y.-Z. Zhang, D.-F. Li, R. Clérac, S.M. Holmes, Polyhedron 60 (2013) 110–115.
[21] D. Li, S. Parkin, G. Wang, G.T. Yee, S.M. Holmes, Inorg. Chem. 45 (2006) 2773.
[22] A. Brown, M. Saber, W. Van den Heuvel, K. Schulte, A. Soncini, K.R. Dunbar, Inorg. Chem. 56 (2017) 1031.
[23] Y.-Z. Zhang, D.-F. Li, R. Clérac, S.M. Holmes, Polyhedron 60 (2013) 110.
[24] C.C. Beedle, Y.-Z. Zhang, S.M. Holmes, S. Hill, S. Polyhedron 59 (2013) 48.
[25] R. Clérac, H. Miyasaka, M. Yamashita, C. Coulon, J. Am. Chem. Soc. 124 (2002) 12837.
[26] L.M. Toma, R. Lescouëzec, S. Uriel, R. Llusar, C. Ruiz-Pérez, J. Vaissermann, F. Lloret, M. Julve, Dalton Trans. (2007) 3690.
[27] T.D. Harris, M.V. Bennett, R. Clérac, J.R. Long, J. Am. Chem. Soc. 132 (2010) 3980.
[28] T. Liu, Y.-J. Zhang, S. Kanegawa, O. Sato, J. Am. Chem. Soc. 132 (2010) 8250.
[29] T. Liu, H. Zheng, S. Kang, Y. Shiota, S. Hayami, M. Mito, O. Sato, K. Yoshizawa, S. Kanegawa, D.A. Chunying, Nat. Comm. 4 (2013) 2826.
[30] M.-G. Alexandru, D. Visinescu, N. Marino, G. de Munno, F. Lloret, M. Julve, RSC Adv. 5 (2015) 95410.
[31] Y.-J. Zhang, T. Liu, S. Kanegawa, O. Sato, J. Am. Chem. Soc. 132 (2010) 912.
[32] K.E. Funck, M.G. Hilfiger, C.P. Berlinguette, M. Shatruk, W. Wernsdorfer, K.R. Dunbar, Inorg. Chem. 48 (2009) 3438, and references cited therein.
[33] D.-F. Li, R. Clérac, O. Roubeau, E. Harté, C. Mathonière, R. Le Bris, S.M. Holmes, J. Am. Chem. Soc. 128 (2008) 252.
[34] Y.-Z. Zhang, D.-F. Li, R. Clérac, M. Kalisz, C. Mathonière, S.M. Holmes, Angew. Chem., Int. Ed. 49 (2010) 3752.
[35] M. Nihei, Y. Sekine, N. Suganami, H. Oshio, Chem. Lett. 39 (2010) 978.
[36] S. Ohkoshi, K. Imoto, Y. Tsunobuchi, S. Takano, H. Tokoro, Nat. Chem. 3 (2011) 564.
[37] M.A. Halcrow, K.R. Dunbar, C. Achim, M. Shatruk, Charge Transfer-Induced Spin-Transitions in Cyanometalate Materials, Wiley, New York, 2013, and references cited therein.
[38] Y.-Z. Zhang, P. Ferko, D. Siretanu, R. Ababei, N.P. Rath, M.J. Shaw, R. Clérac, C. Mathonière, S.M. Holmes, J. Am. Chem. Soc. 136 (2014) 16854.
[39] C. Mathonière, Eur. J. Inorg. Chem. (2018) 248.
[40] O. Sato, T. Iyoda, A. Fujishima, K. Hashimoto, Science 272 (1996) 704.
[41] O. Sato, Y. Einaga, T. Iyoda, A. Fujishima, K. Hashimoto, Inorg. Chem. 38 (1999) 4405.
[42] V. Escax, A. Bleuzen, C. Cartier dit Moulin, F. Villain, A. Goujon, F. Varret, M. Verdaguer, J. Am. Chem. Soc. 123 (2001) 12536.
[43] G. Champion, V. Escax, C. Cartier dit Moulin, A. Bleuzen, F. Villain, F. Baudelet, E. Dartyge, M. Verdaguer, J. Am. Chem. Soc. 123 (2001) 12544.
[44] O. Sato, Acc. Chem. Res. 36 (2003) 692, and references cited therein.
[45] A. Bleuzen, V. Marvaud, C. Mathonière, B. Sieklucka, M. Verdaguer, Inorg. Chem. 48 (2009) 3453, and references cited therein.
[46] J.T. Culp, J.-H. Park, M.W. Meisel, D.R. Talham, Polyhedron (2003) 3059.
[47] L. Catala, T. Mallah, Coord. Chem. Rev. 346 (2018) 32.
[48] Y. Prado, S. Mazerat, E. Rivière, G. Rogez, A. Gloter, O. Stéphan, L. Catala, T. Mallah, Adv. Funct. Mater. 24 (2014) 5402.
[49] Y. Prado, M.-A. Arrio, F. Volatron, E. Otero, C. Cartier dit Moulin, P. Sainctavit, L. Catala, L. Mallah, Chem. Eur. J. 19 (2013) 6685.
[50] M.K. Peprah, C.H. Li, D.R. Talham, M.W. Meisel, Polyhedron 66 (2013) 264.
[51] A.S. Felts, A. Slimani, J.M. Cain, M.J. Andrus, A.R. Ahir, K.A. Abboud, M.W. Meisel, K. Boukheddaden, D.R. Talham, J. Am. Chem. Soc. 140 (2018) 5814.
[52] Y. Moritomo, K. Kato, A. Kuriki, M. Takata, M. Sakata, H. Tokoro, S. Ohkoshi, K. Hashimoto, J. Phys. Soc. Jpn. 71 (2002) 2078.
[53] E.J.M. Vertelman, T.T.A. Lummen, A. Meetsma, M.W. Bouwkamp, G. Molnar, P. H.M. van Loosdrecht, P.J. van Konigsbruggen, Chem. Mater. 20 (2008) 1236.
[54] G. Molnár, S. Cobo, T. Mahfoud, E.J.M. Vertelman, P.J. van Konigsbruggen, P. Demont, A. Bousseksou, J. Chem. Phys. C 113 (2009) 2586.
[55] J.-H. Her, P.W. Stephens, C.M. Kareis, J.S. Moore, K.S. Min, J.-W. Park, G. Bali, B.S. Kennon, J.S. Miller, Inorg. Chem. 49 (2010) 1524.
[56] H. Tokoro, S.-I. Ohkoshi, Dalton Trans. 40 (2011) 6825, and references cited therein.
[57] S.-I. Ohkoshi, H. Tokoro, Acc. Chem. Res. 45 (2012) 1749.
[58] C. Tian, E. Kan, C. Lee, M.-H. Whangbo, Inorg. Chem. 49 (2010) 3086.
[59] Z.H. Ni, H.Z. Kou, Y.H. Zhao, L. Zheng, R.J. Wang, A.L. Cui, O. Sato, Inorg. Chem. 44 (2005) 2050.
[60] M. Ferbinteanu, H. Miyasaka, W. Wernsdorfer, K. Nakata, K.-I. Sugiura, M. Yamashita, C. Coulon, R. Clérac, J. Am. Chem. Soc. 127 (2005) 3090.
[61] H.R. Wen, C.F. Wang, Y. Song, S. Gao, J.L. Zuo, X.Z. You, Inorg. Chem. 45 (2006) 8942.
[62] L. Jiang, X.L. Feng, T.B. Lu, S. Gao, Inorg. Chem. 45 (2006) 5018.
[63] L.M. Toma, R. Lescouëzec, J. Pasán, C. Ruiz-Pérez, J. Vaissermann, J. Cano, R. Carrasco, W. Wernsdorfer, F. Lloret, M. Julve, J. Am. Chem. Soc. 128 (2006) 4842.
[64] D. Zhang, H. Wang, Y. Chen, Z.-H. Ni, L. Tian, J. Jiang, Inorg. Chem. 48 (2009) 5488.
[65] L.M. Toma, J. Pasán, C. Ruiz-Pérez, F. Lloret, M. Julve, Dalton Trans. 41 (2012) 13716.
[66] A. Panja, P. Guionneau, I.-R. Jeon, S.M. Holmes, R. Clérac, C. Mathonière, Inorg. Chem. 51 (2013) 12350.
[67] D. Dong, Y. Zhang, C. Jiao, L. Zhao, T. Liu, D. Liu, Z. Li, J. Liu, D. Liu, New J. Chem. 40 (2016) 8451.
[68] E.A. Boudreaux, L.N. Mulay, Theory and Applications of Molecular Paramagnetism, Wiley, NY, 1976, pp. 491–496.
[69] G.M. Sheldrick, SHELX-97, Programs for Crystal Structure Solution and Refinement, University of Göttingen, Göttingen, Germany
[70] G.M. Sheldrick, Acta Crystallogr. A 64 (2008) 112.
[71] G.M. Sheldrick, SADABS, An empirical absorption correction program, Bruker Analytical X-ray Systems, Madison, WI, 1996
[72] International Tables for Crystallography, vol. C, Kluwer Academic Publishers, Dordrecht, Netherlands, 1992.
[73] S.R. Choudhury, A. Dutta, S. Mukhopadhyay, L.P. Lu, M.L. Zhu, Acta Cryst. E 62 (2006) m1489.
[74] S.A. Richert, P.K.S. Tsang, D.T. Sawyer, Inorg. Chem. 28 (1989) 2471.
[75] J.A. Smith, J.-R. Galán-Mascarós, R. Clérac, J.-S. Sun, X. Ouyang, K.R. Dunbar, Polyhedron 20 (2001) 1727.
[76] S.R. Holleman, O.J. Parker, G.L. Breneman, Acta Cryst. C50 (1994) 867.
[77] M. Wang, J. England, T. Weyermüeller, K. Weighardt, Inorg. Chem. 53 (2014) 2276.
[78] J. Goodenough, Magnetism and the Chemical Bond, Wiley, New York, 1963.
[79] J.J. Borrás-Almenar, J.M. Clemente-Juan, E. Coronado, B.S. Tsukerblat, Inorg. Chem. 38 (1999) 6081.
[80] J.J. Borrás-Almenar, J.M. Clemente-Juan, E. Coronado, B.S. Tsukerblat, J. Comput. Chem. 22 (2001) 985.